Metabolic Engineering 45 (2018) 86–94

Contents lists available at ScienceDirect

Metabolic Engineering

journal homepage: www.elsevier.com/locate/meteng

Controlling cell-free metabolism through physiochemical perturbations

Ashty S. Karim[a,b,c,1], Jacob T. Heggestad[a,b,c,1], Samantha A. Crowe[a,b,c,1], Michael C. Jewett[a,b,c,d,e,*,1]

[a] Department of Chemical and Biological Engineering, Northwestern University, Evanston, IL 60208, USA
[b] Chemistry of Life Processes Institute, Northwestern University, Evanston, IL 60208, USA
[c] Center for Synthetic Biology, Northwestern University, Evanston, IL 60208, USA
[d] Robert H. Lurie Comprehensive Cancer Center, Northwestern University, Chicago, IL 60611, USA
[e] Simpson Querrey Institute, Northwestern University, Chicago, IL 60611, USA

ARTICLE INFO

Keywords:
Cell-free
CFPS
Butanol
Cofactors
NAD
Liquid-handling robotics

ABSTRACT

Building biosynthetic pathways and engineering metabolic reactions in cells can be time-consuming due to complexities in cellular metabolism. These complexities often convolute the combinatorial testing of biosynthetic pathway designs needed to define an optimal biosynthetic system. To simplify the optimization of biosynthetic systems, we recently reported a new cell-free framework for pathway construction and testing. In this framework, multiple crude-cell extracts are selectively enriched with individual pathway enzymes, which are then mixed to construct full biosynthetic pathways on the time scale of a day. This rapid approach to building pathways aids in the study of metabolic pathway performance by providing a unique freedom of design to modify and control biological systems for both fundamental and applied biotechnology. The goal of this work was to demonstrate the ability to probe biosynthetic pathway performance in our cell-free framework by perturbing physiochemical conditions, using *n*-butanol synthesis as a model. We carried out three unique case studies. First, we demonstrated the power of our cell-free approach to maximize biosynthesis yields by mapping physiochemical landscapes using a robotic liquid-handler. This allowed us to determine that NAD and CoA are the most important factors that govern cell-free *n*-butanol metabolism. Second, we compared metabolic profile differences between two different approaches for building pathways from enriched lysates, heterologous expression and cell-free protein synthesis. We discover that phosphate from PEP utilization, along with other physiochemical reagents, during cell-free protein synthesis-coupled, crude-lysate metabolic system operation inhibits optimal cell-free *n*-butanol metabolism. Third, we show that non-phosphorylated secondary energy substrates can be used to fuel cell-free protein synthesis and *n*-butanol biosynthesis. Taken together, our work highlights the ease of using cell-free systems to explore physiochemical perturbations and suggests the need for a more controllable, multi-step, separated cell-free framework for future pathway prototyping and enzyme discovery efforts.

1. Introduction

Building and optimizing biosynthetic pathways in cells offers promising solutions to problems in energy and medicine but is often time-consuming (Keasling, 2012, 2010; Nielsen and Keasling, 2016). This is, in part, because pathway construction involves designing and tuning DNA cassettes to balance heterologous enzyme expression levels, selecting the best enzymes for the desired chemistries, and engineering native metabolic pathways to channel flux towards the desired product (Nielsen and Keasling, 2016; Paddon and Keasling, 2014). In addition, enzyme candidates from databases (like BRENDA, (Chang et al., 2015) METACYC (Caspi et al., 2014), *etc.*) containing thousands of enzyme variants with available kinetic data must be selected and tested. However, with even the most informed selection process, it may be that the selected enzymes do not have the desired properties for a particular biosynthesis (Lee et al., 2012; Na et al., 2010). With the current metabolic engineering Design-Build-Test (DBT) cycle time being on the order of weeks to months to test a given pathway configuration, it can take hundreds of person-years of research and development time to test the number of enzyme and pathway variants needed to bring a biochemical to market (Paddon and Keasling, 2014; Boyle and Silver, 2012; Kwok, 2010).

* Correspondence to: Department of Chemical and Biological Engineering, Northwestern University, Evanston, IL 60208, USA.
E-mail address: m-jewett@northwestern.edu (M.C. Jewett).
[1] Postal address: 2145 Sheridan Road, Tech E-136, Evanston, IL 60208, USA.

https://doi.org/10.1016/j.ymben.2017.11.005
Received 26 May 2017; Received in revised form 3 November 2017; Accepted 11 November 2017
Available online 15 November 2017

Cell-free systems provide many advantages for accelerating DBT cycles and probing metabolism (Dudley et al., 2015; Morgado et al., 2016; Dong et al., 2015). For example, the open reaction environment allows direct monitoring and manipulation of the system to study pathway performance. As a result, many groups have used purified enzyme systems to study enzyme kinetics and inform cellular expression (Dudley et al., 2015; Bogorad et al., 2013; Zhu et al., 2014). Recently, the Liao group showed that cell-free pathways could be used as a tool to successfully develop a non-oxidative glycolytic pathway that maximizes carbon utilization in *Escherichia coli* whole cells (Bogorad et al., 2013). Despite advances in purified enzyme systems, crude lysates are becoming an increasingly popular alternative to build biosynthetic pathways because they inherently provide the context of native-like metabolic networks (Karim and Jewett, 2016; Dudley et al., 2016; Hold et al., 2016; Bujara et al., 2011).

The presence of native metabolic enzymes and cofactor regeneration in crude lysates (Jewett and Swartz, 2004) allows for observations of metabolic interactions with biosynthetic pathways, which is limited in purified systems (Dudley et al., 2015). For instance, the Panke group has shown that DHAP can be made in crude lysates and real-time monitoring can optimize production (Hold et al., 2016; Bujara et al., 2011). In addition, our group has shown that 2,3-butanediol (Kay and Jewett, 2015), mevalonate (Dudley et al., 2016), *n*-butanol (Karim and Jewett, 2016), and more complex products (Goering et al., 2016) can be constructed in crude lysates with high productivities (> g/L/h). In these systems, removing cell growth requirements reduces the complexity of the metabolic reactions that could interact with the expression of a biosynthetic pathway while maintaining native energy metabolism active. Crude lysates also have the capability to construct biosynthetic pathways by expressing enzymes directly *in vitro* by cell-free protein synthesis (CFPS) (*in vitro* transcription and translation) (Karim and Jewett, 2016; Goering et al., 2016).

Producing chemicals and testing biosynthetic pathways *via* crude lysate metabolic engineering is quick and efficient. In our recent work (Karim and Jewett, 2016) with the CoA-dependent *n*-butanol pathway (Fig. 1**A**), we developed a cell-free framework to study metabolic pathways. In our framework, cell-free cocktails for synthesizing target small molecules are assembled in a mix-and-match fashion from selectively enriched crude-cell lysates containing pathway enzymes either from heterologous overexpression prior to lysis (Fig. 1**B**) or from direct *in vitro* production by CFPS (Fig. 1**C**). Incorporating CFPS as a means of enzyme production reduces the time to build pathways and test heterologous enzymes. However, coupling CFPS with crude extract mixing for building biosynthetic pathways (CFPS-ME) underperforms in the context of *n*-butanol production titers, yields and productivities as compared to the mix-and-match pre-enriched lysates (CFME) approach.

It would be beneficial if we could probe how native metabolism and heterologous pathways interact in crude lysates through physiochemical alterations both to understand why CFPS-ME underperforms and to increase the utility of the cell-free platform to study cellular metabolism and biosynthesis. We would be able to study how enzymes might synergize with each other and identify ratios of enzymes (Dudley et al., 2016) necessary for optimal pathway performance. We could learn which regimes of metabolism in cell-free might mimic or relate to cellular environments. Additionally, we could probe enzyme inhibition mechanisms by manipulation of the physiochemical environments.

In this work, we set out to demonstrate the ability to probe biosynthetic pathway performance through physiochemical parameters, using cell-free *n*-butanol synthesis as a model. The key idea was to show that we could rapidly explore and influence cell-free pathway performance by varying unique combinations of substrates, cofactors, salts, buffers, *etc.,* in crude extract-based cell-free biotransformations. We specifically carried out three distinct case studies focused on how by-products evolve over the time of a reaction. First, we wanted to demonstrate that such studies could be enabled using robotic liquid-handling systems to access combinatorial design space that exceeds typical pipelines pursued in cells. By testing 40 different reaction conditions in one day, we identified NAD and CoA as the two most important parameters controlling cell-free *n*-butanol biosynthesis and improved titers 9.3 ± 2.3 fold as compared to our starting conditions. We then generated cofactor landscape maps that identify optimum cofactor ratios for pathway performance. Second, we wanted to rigorously study why and how we might mitigate the underperformance of CFPS-coupled crude-lysate metabolic systems to better understand how these systems can be used to rapidly prototype biosynthetic pathways. Third, we wanted to show that different energy sources could be used to fuel CFPS and cell-free *n*-butanol production to relieve phosphate toxicity. Taken together, our results show that cell-free systems enable combinatorial and modular assembly of pathways to improve pathway performance using well-defined experimental conditions. They also set the stage for the development of a multi-step, separated CFPS-coupled cell-free metabolic engineering framework for controlled enzyme and biosynthetic pathway study.

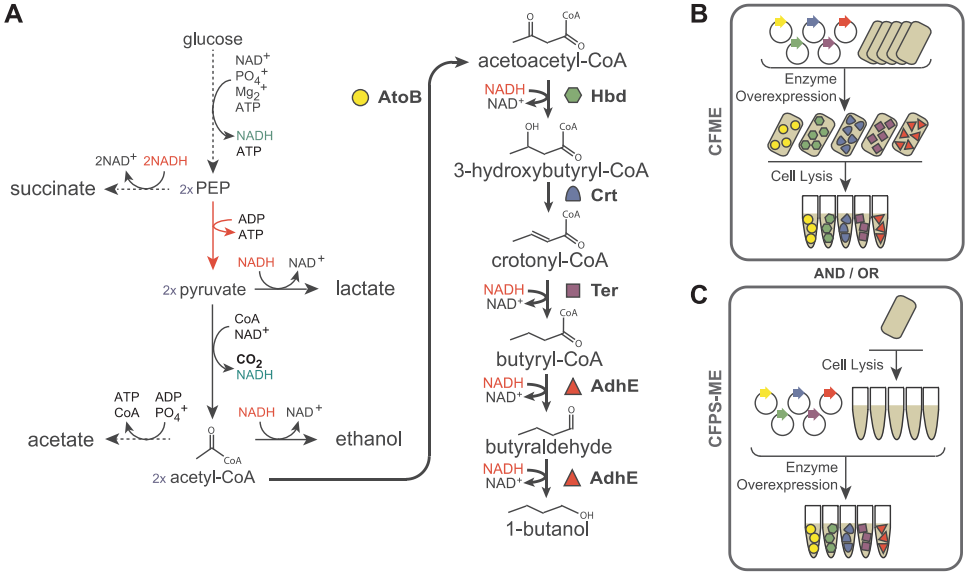

Fig. 1. A schematic for cell-free expression of a *n*-butanol model pathway. (**A**) Schematic representation of the constructed biosynthetic *n*-butanol pathway. Acetyl-CoA is generated through *E. coli*'s natural glycolysis and funneled into the *C. acetobutylicum*-derived CoA-dependent pathway to produce *n*-butanol. Major by-products and cofactors are shown. Heterologous enzymes used are as follows: AtoB (*Escherichia coli*), Hbd (*Clostridium beijerinckii, CB*), Crt (*Clostridium acetobutylicum, CA*), Ter (*Treponema denticola, TD*), AdhE (*Clostridium acetobutylicum, CA*). Methodologies for enzyme production for (**B**) cell-free metabolic engineering (CFME) and (**B**) cell-free protein synthesis driven metabolic engineering (CFPS-ME) are depicted.

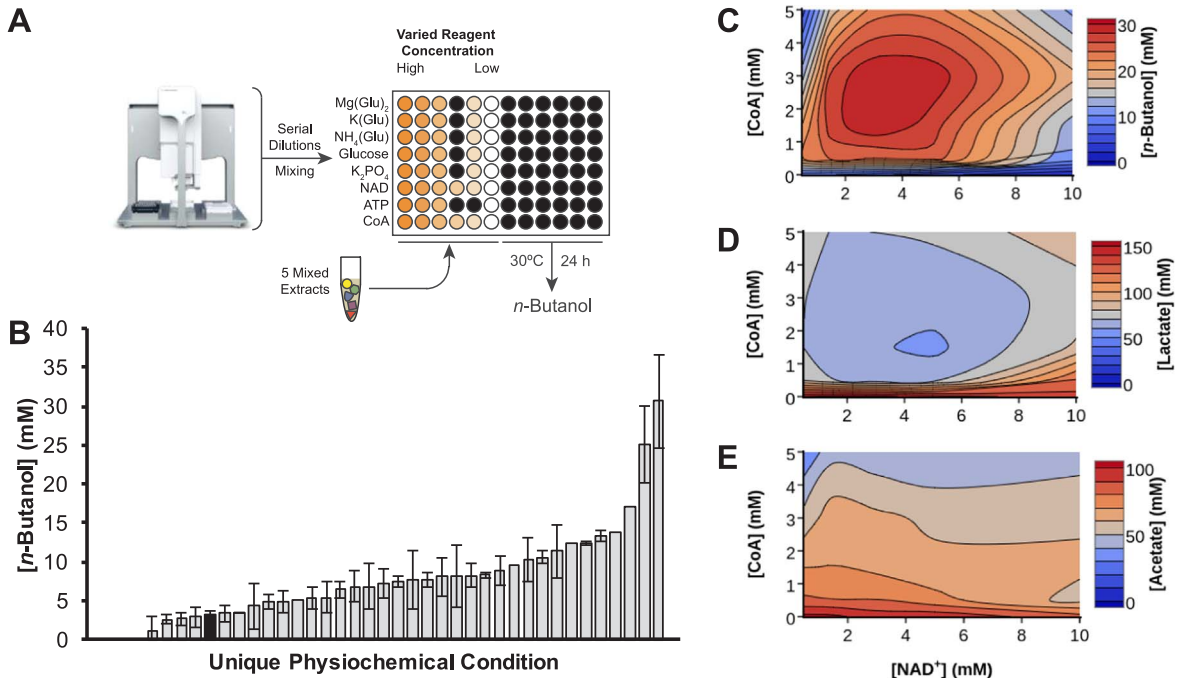

Fig. 2. Liquid-handling robotics guide physiochemical optimizations of cell-free *n*-butanol metabolism. (**A**) Design of liquid-handling robotic reaction set up is shown. (**B**) The fitness of each unique physiochemical condition is represented as concentration of *n*-butanol after 24 h incubation at 30 °C. Each bar corresponds to the physicochemical conditions in the order listed in Supplementary Table 1. Error bars represent average error of technical replicates with n = 2. The black bar represents base case condition. Based on (**B**), the concentration of CoA was varied between zero and five mM and the concentration of NAD was varied between zero and ten mM. The concentrations after 24 h incubation at 30 °C of (**C**) *n*-butanol, (**D**) lactate, and (**E**) acetate were measured. The average concentration of three technical replicates was graphed.

2. Material and methods

2.1. Bacterial strains and plasmids

Both *E. coli* DH5α and NEB Turbo™ (NEB) were used for plasmid preparation. *E. coli* BL21(DE3) (NEB) was used for protein overexpression and for preparation of all extracts. A modified version of pET-22b (Novagen/EMD Millipore), used in previous studies (Karim and Jewett, 2016; Kay and Jewett, 2015), was used for all constructs for *in vivo* overexpression of proteins. For *in vitro* expression of proteins, the pJL1 vector was used. Carbenicillin (100 μg ml^{-1}) was used with the pET vector system and kanamycin (50 μg ml^{-1}) was used with the pJL1 vector system. Propagated constructs were purified using an EZNA Plasmid Mini Kit (Omega Bio-Tek). All plasmids used in this study were used in our previous studies (Karim and Jewett, 2016).

2.2. Cell extract preparation

E. coli BL21(DE3) cells were grown in 2 × YTPG media (16 g l^{-1} tryptone, 10 g l^{-1} yeast extract, 5 g l^{-1} NaCl, 7 g l^{-1} potassium phosphate monobasic, 3 g l^{-1} potassium phosphate dibasic, 18 g l^{-1} glucose). These cells were cultured at the 50 ml scale in 250 ml baffled tunair shake flasks (IBI Scientific, Peosta, IA) and at the 1 L scale in a 37 °C incubator with shaking at 250 rpm. When cells reached OD_{600} = 0.6–0.8, the cultures were induced with 0.1 mM IPTG. After induction cultures were grown for 4 h at 30 °C when plasmid expression was required and grown to OD_{600} = 3.0 for plasmid-less extracts. Antibiotics were not used during cell growth. The cells were harvested by centrifugation at 8000*g* at 4 °C for 15 min and were washed two times with cold S30 buffer (10 mM Tris-acetate (pH 8.2), 14 mM magnesium acetate, and 60 mM potassium glutamate). After final wash and centrifugation, the pelleted wet cells were weighed, flash frozen in liquid nitrogen, and stored at − 80 °C. The thawed cells were suspended in 0.8 ml of S30 buffer per 1 g of wet cell mass. In order to lyse cells by sonication, thawed and suspended cells were transferred into 1.5 ml microtube and placed in an ice-water bath to minimize heat damage during sonication. The cells were lysed using a Q125 Sonicator (Qsonica, Newtown, CT) with 3.175 mm diameter probe at frequency of 20 kHz and 50% of amplitude. The input energy (Joules) was monitored and 830 J was used for 1.4 ml of suspended cells Kwon and Jewett (2015). The lysate was then centrifuged at 12,000*g* at 4 °C for 10 min. All of prepared cell extracts were flash frozen in liquid nitrogen and stored at − 80 °C until use. Quick-Start Bradford protein assay kits (Bio-Rad) were used to measure the total protein concentration of each extract with a bovine serum albumin standard.

2.3. CFME reactions

Reactions were carried out in 1.5 ml Eppendorf tubes at 37 °C in 25 μl volumes. Each reaction consisted of mixing five extracts, containing one enzyme overexpressed each, to complete the biosynthetic *n*-butanol pathway (2 mg ml^{-1}) along with magnesium glutamate (8 mM), ammonium glutamate (10 mM), potassium glutamate (134 mM), glucose (120 mM), dipotassium phosphate (10 mM, pH 7.2), Bis Tris (100 mM), NAD (3 mM), and CoA (1.5 mM), unless otherwise noted. Reactions were terminated by adding 5% w/v trichloroacetic acid in a 1:1 ratio. Precipitated proteins were pelleted by centrifugation at 21,000*g* for 10 min at 4 °C. The supernatant was stored at − 80 °C until analysis.

2.4. Liquid-handling robotics

An Agilent BRAVO liquid-handling robot (Agilent Technologies) was used to carry out the reaction setup for select CFME reactions. The liquid-handling workstation has nine plate decks and a 96-pipette tip head movable in the x-y-z directions. The workstation was programmed using VWorks™ Automation Control Software (BioNex Solutions, Inc.) to pipette different arrangements of reagents. Each CFME reagent (magnesium glutamate, ammonium glutamate, potassium glutamate, glucose, dipotassium phosphate, NAD, ATP, and CoA) was diluted to

five different concentrations using dH_2O and stock solutions in a 96-well plate. Each component was then pooled together into one well on a new plate so that each well in the new plate contained all eight components at standard concentrations except one reagent that was varied at a time (Fig. 2**A**). Therefore, the new plate contained 40 wells with one unique reagent and concentration tested in each. CFME mixed extracts containing the full *n*-butanol pathway were then added to each well. All reaction conditions set up are listed in Supplementary Table 1.

2.5. CFPS-ME reactions

CFPS reactions were performed to express enzymes involved in *n*-butanol production prior to starting the CFME portion of the reactions using a modified PANOx-SP system Jewett and Swartz (2004). A 25 µl CFPS reaction in a 1.5 ml microcentrifuge tube was prepared by mixing the following components: ATP (1.2 mM); GTP, UTP, and CTP (0.85 mM each); folinic acid (34.0 µg ml^{-1}); *E. coli* tRNA mixture (170.0 µg ml^{-1}); 20 standard amino acids (2 mM each); nicotinamide adenine dinucleotide (NAD; 0.33 mM); coenzyme-A (0.27 mM); spermidine (1.5 mM); putrescine (1 mM); potassium glutamate (130 mM); ammonium glutamate (10 mM); magnesium glutamate (12 mM); phosphoenolpyruvate (PEP; 33 mM), and cell extract (~ 12 mg ml^{-1}). For each reaction plasmid was added at ~ 13.3 or ~ 26.6 µg ml^{-1}. Reactions were incubated at 30 °C for 3 h. The *n*-butanol production portion of the reaction was initiated by supplementing glucose (120 mM) and additional reagents (3 mM NAD and 1.5 mM CoA final concentrations) noted throughout the manuscript and were incubated at 30 °C for 24 h. The final concentration of cofactors in Fig. 3 CFPS-ME reactions was 0.3 mM NAD and 1.5 mM CoA, matching CFPS-ME reaction conditions previously published Karim and Jewett (2016). The total extract concentration during the *n*-butanol production portion of the reaction is 10 mg ml^{-1}, the same as a CFME reaction.

2.6. GFP quantification

Superfolder GFP (sfGFP) is a reporter protein used during CFPS from the plasmid pJL1-sfGFP. Active sfGFP protein yields were quantified by measuring fluorescence. Two microliters of CFPS reaction was added in the middle of the flat bottom of 96-well half area black plates (Costar 3694; Corning Incorporated, Corning, NY). sfGFP was excited at 485 nm while measuring emission at 528 nm with a 510 nm cutoff filter. The fluorescence of sfGFP was converted to concentration (µg ml^{-1}) according to a standard curve (Hong et al., 2014).

2.7. Quantification of metabolites

High-performance liquid chromatography (HPLC) was used to analyze glucose, lactate, acetate, and *n*-butanol in the reactions. The metabolites were measured with an Agilent 1260 series HPLC system (Agilent, Santa Clara, CA) *via* a refractive index (RI) detector. Analytes were separated using an Aminex HPX-87H anion exchange column (Bio-Rad Laboratories) with a 5 mM sulfuric acid mobile phase at 55 °C and a flow rate of 0.6 ml min^{-1}. Commercial standard of each metabolite was used for quantification of experimental samples by linear interpolation of external standard curves.

3. Results

The goal of this work was to demonstrate the ability to rapidly explore and influence cell-free metabolism and *n*-butanol synthesis by varying unique combinations of physiochemical parameters in three ways. First, we tested the effect of each small molecule reagent added to the cell-free system on cell-free *n*-butanol production with enzymes pre-enriched by heterologous expression (CFME) and optimized the small molecule conditions to increase *n*-butanol production. Second, we compared the metabolic profiles of our CFME system with that of the CFPS-coupled system (CFPS-ME) and tested the individual effect of each reagent used during CFPS on *n*-butanol synthesis. Third, we attempted to mitigate negative effects of CFPS by using non-phosphorylated secondary energy substrates to fuel cell-free protein synthesis and *n*-butanol biosynthesis.

3.1. Changes in NAD and CoA greatly contribute to changes in metabolism

We first carried out a series of optimization experiments to assess the impact of small molecule solutes on CFME *n*-butanol biosynthesis activity. The CFME reaction contains five mixed lysates pre-enriched with each individual *n*-butanol pathway enzyme (Fig. 1**B**) along with

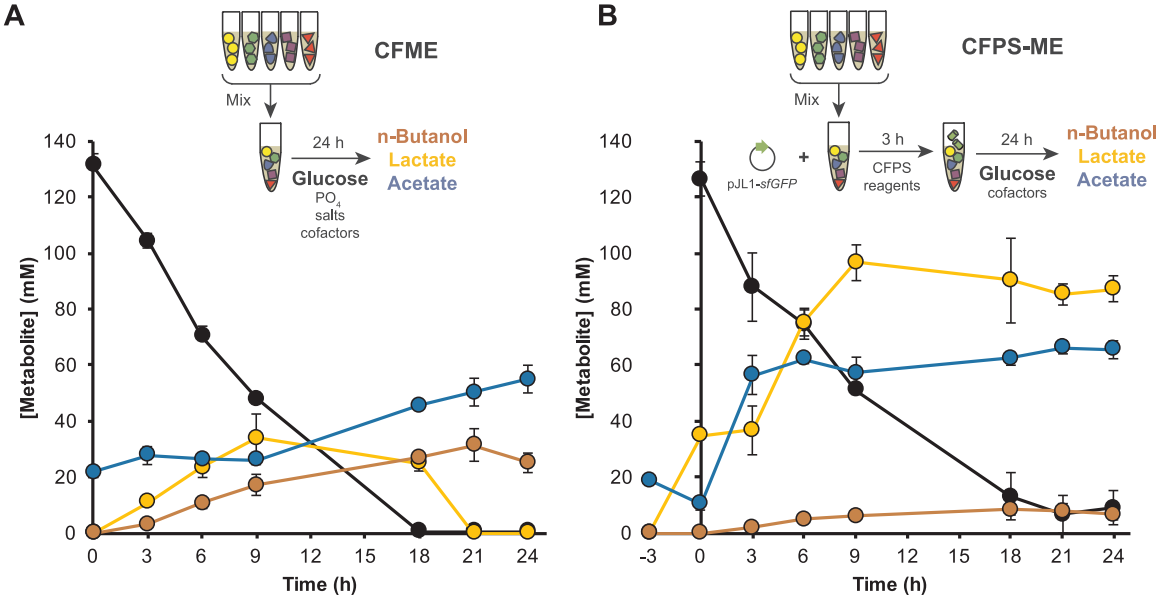

Fig. 3. Protein synthesis alters cell-free metabolism and decreases *n*-butanol production. Cell-free reactions were run for 24 h at 30 °C and glucose (black), lactate (yellow), acetate (blue), and *n*-butanol (orange) were measured. (**A**) CFME reactions are run with five extracts mixed to have all *n*-butanol pathway enzymes present with glucose, NAD (3 mM), and CoA (1.5 mM). (**B**) CFPS-ME is run the same way with a 3 h incubation period with DNA and CFPS components prior to addition of glucose and CoA (1.5 mM). Each error bar represents standard deviations of technical replicates with n ≥ 3. (For interpretation of the references to color in this figure legend, the reader is referred to the web version of this article.)

substrates, cofactors, and salts designed to mimic the cytoplasmic environment. Specifically, we explored the effects salt concentration (*i.e.*, magnesium glutamate, potassium glutamate, and ammonium glutamate), glucose concentration, cofactor concentration (*e.g.,* NAD, CoA), phosphate concentration, and ATP concentration on *n*-butanol synthesis. While we know the approximate concentrations of each of these components in *E. coli* cells (Supplementary Table 2), varying the concentration of these components could provide insight into pathway operation. We used a robotic liquid-handling system to vary the concentrations of these eight chemical reagents (Fig. 2**A**). The robot first makes serial dilutions of each of the eight components. Then, the robot pools the reagent dilutions into 40 unique physiochemical environments (Supplementary Table 1). To initiate *n*-butanol synthesis, the mixed extract is then added to each physiochemical condition. Reactions are incubated at 30 °C in 96-well plates. Fig. 2**B** shows the amount of *n*-butanol produced at 24 h in the 40 unique physiochemical conditions tested. The variability in technical replicates is due to accuracy of pipetting by the liquid-handler. In a single pass, we were able to increase *n*-butanol titers 9.3 ± 2.3 fold as compared to our originally reported CFME system conditions (black bar). This result highlights the potential power of cell-free systems to rapidly optimize pathway performance.

We next set out to understand the reason for increased *n*-butanol yields. We found that the top 3 conditions corresponded to high levels of initial NAD, holding all other components constant, resulting in a statistically significant increase in *n*-butanol produced ($p = 0.025$). On the lower end, the four conditions that produced 0 mM *n*-butanol were a result of conditions with (1) no glucose added, (2) no NAD, and (3 & 4) high levels of CoA. This analysis not only served as an important control, because as expected *n*-butanol was not synthesized in the absence of glucose, but it also pointed to NAD as the most important added reagent positively correlated with high-level *n*-butanol production. Our results are consistent with the requirement of four molecules of NADH to produce one molecule *n*-butanol in the pathway (Fig. 1**A**). Varying amounts of CoA is also a lever to control *n*-butanol metabolism, though it appeared from our initial screen that CoA levels would need to be finely tuned.

Given the freedom of design in adjusting cell-free system components, we further explored the synergistic effects of varying NAD (0–10 mM) and CoA (0–5 mM) concentrations, while keeping all other components constant, on *n*-butanol synthesis. This strategy allows us to rapidly map cofactor landscapes to explore local and global optima. We observed that pathway performance is carefully tuned, with an optimal balance between amounts of NAD and CoA needed to achieve the highest *n*-butanol values (Fig. 2**C**). Our results suggest that when CoA and NAD are low, the flux through the acetyl-CoA node and the redox driving force to *n*-butanol are limited. When there is too much NAD or CoA present, flux likely is diverted to other nodes. To test this, we directly measured lactate (Fig. 2**D**) and acetate (Fig. 2**E**) production in the CFME reactions at 24 h. Lactate produced from pyruvate and acetate produced from acetyl-CoA, are two major by-products of cell-free *n*-butanol metabolism. We observed that acetate is inversely dependent on the starting concentration of CoA in the reaction and not dependent as much on NAD concentration. Acetate production is probably linked to CoA because the phosphotransacetylase and acetate kinase reactions convert acetyl-CoA to acetate and ATP while recycling phosphate. However, lactate has a similar optimal NAD to CoA ratio as *n*-butanol. Taken together, our results show that the cell-free framework and its barrier-free access to reaction conditions is well-suited for rapidly acquiring physiochemical landscapes to assess and optimize biosynthetic pathway performance. This joins an emerging body of literature highlighting the value of cell-free systems for prototyping biological systems (Hold et al., 2016; Garamella et al., 2016; Takahashi et al., 2015; Sun et al., 2014; Kelwick et al., 2016; Moore et al., 2017).

3.2. Cell-free metabolic profiles are negatively affected by CFPS integration

Cell-free protein synthesis as a means of direct *in vitro* production of biosynthetic enzymes for crude-lysate metabolic engineering efforts (Fig. 1**C**) enables faster DBT cycle times (Karim and Jewett, 2016). Unfortunately, we observed in our previous work that the yields of *n*-butanol in CFPS-ME reactions were lower than in CFME reactions (where biosynthesis enzymes are made in cells before extracts are made) (Karim and Jewett, 2016). We thus set out to exploit the flexibility afforded by *in vitro* systems to modulate physiochemical conditions for systematically studying these differences and to demonstrate the ease of studying pathway performance in cell-free systems. Detailed quantification revealed how changes in glucose, lactate, acetate, and *n*-butanol varied for CFME (Fig. 3**A**) and CFPS-ME (Fig. 3**B**) over the course of a 24 h reaction at 30 °C. We observed three distinct regimes: (i) 0–3 h, (ii) 3–9 h, and (iii) 9+ h. During the first regime, there is a "lag" phase where glucose is consumed and metabolism starts up, making NADH. During the second regime, all metabolites are produced at a constant rate. The metabolite profiles level off during the third regime.

Several differences between the cell-free metabolite profiles of CFME and CFPS-ME are notable. The two systems consume glucose at similar rates, but CFPS-ME systems produce *n*-butanol at ~ 25% of the titer of CFME systems. Additionally, lactate is produced and then consumed while acetate slowly increases after maximal lactate titer is achieved over the course of the CFME reaction. Whereas in CFPS-ME reactions, acetate and lactate are both only produced. Given the reduction in *n*-butanol yields, we wanted to understand the potential causes for the different metabolic profiles that arise when CFPS is used to make biosynthetic enzymes by directly accessing the physiochemical levers of the cell-free system. We know from our optimizations using liquid-handling robotics (Fig. 2) that NAD and CoA are critical to pathway performance, so it was not surprising that when we compare the original CFPS-ME system (Karim and Jewett, 2016) (Fig. 3**B**) with a CFPS-ME system containing the CFME-optimized NAD and CoA concentrations, we see an improvement in overall *n*-butanol production (Supplementary Fig. 1). However, increasing NAD concentrations still results in *n*-butanol production at ~ 80% of the titer of CFME systems. Therefore, we decided to further explore how CFPS might be affecting biosynthetic performance by directly accessing the physiochemical levers of the cell-free system.

To produce proteins of interest, CFPS systems harness an ensemble of catalytic components necessary for energy generation and protein synthesis from crude lysates of cells. These activated catalysts act as a chemical factory to synthesize and fold desired protein products upon incubation with essential substrates, which include amino acids, nucleotides, DNA or mRNA template encoding the target protein, energy substrates, cofactors, and salts. We hypothesized that the differences we observed in Fig. 3 arose from either (i) changes in the extract that result from protein production or (ii) physiochemical components (which differ than those needed for biosynthetic pathway operation alone). To test which part was responsible, we performed CFME reactions without CFPS, with CFPS small molecule reagents alone, and with a complete CFPS system for sfGFP production prior to the addition of glucose and cofactors (activating *n*-butanol production) and incubation for 24 h at 30 °C (Supplementary Fig. 2). The idea was to understand the impact on cell-free metabolism with and without synthesis of a protein that would not affect the *n*-butanol biosynthesis pathway. We found that *n*-butanol is produced at the same rate and titer in both cases, suggesting that the CFPS reagents alone (or their metabolic byproducts) are most likely the causative factor to the observable metabolic differences.

We then increased the resolution of our study by testing the effect of each of the small molecule CFPS components individually on metabolism (specifically the effect on glucose consumption as well as acetate, lactate, and *n*-butanol production) (Fig. 4**A**). The small molecules unique to CFPS and not involved in CFME can be categorized into three

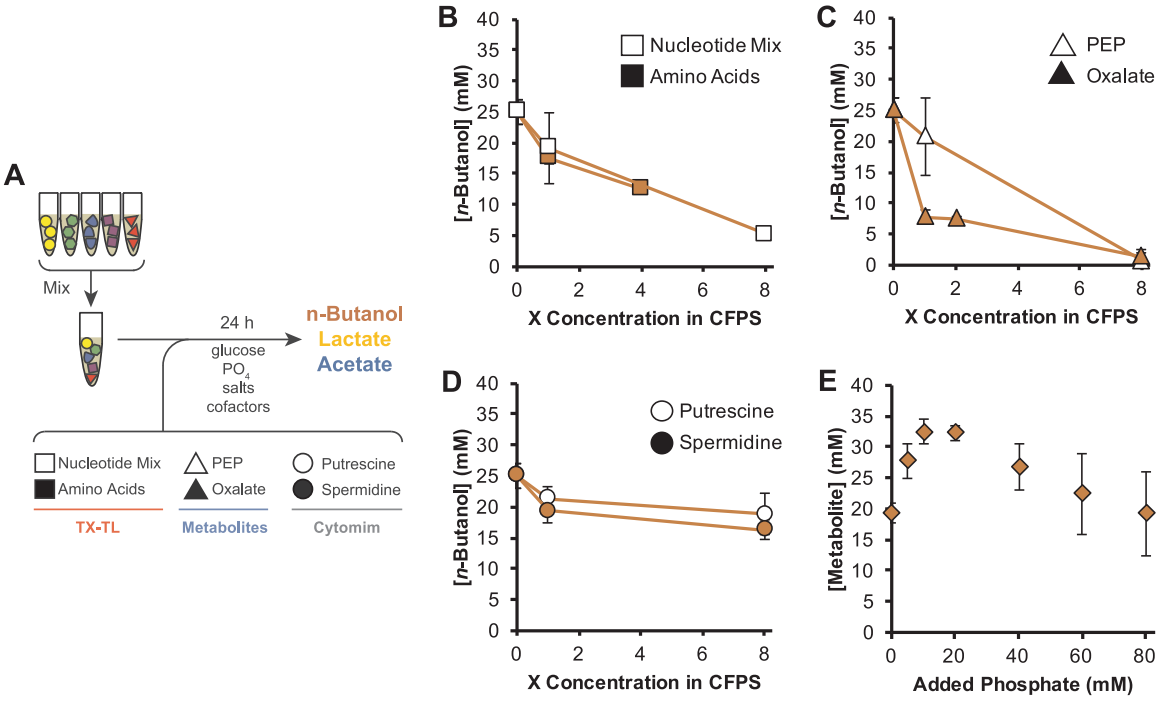

Fig. 4. CFPS components rather than protein synthesis have a greater effect on *n*-butanol synthesis. CFME reactions were run in the presence of individual CFPS reagents for 24 h at 30 °C. (**A**) The design of experiments is represented in schematic form. *n*-Butanol was measured in the presence of varied (**B**) concentrations of transcription-translation specific reagents (TX-TL; nucleotide mix (white squares) and amino acids (orange squares)), **(C)** concentrations of CFPS energy metabolism reagents (Metabolites; PEP (white triangles) and oxalate (orange triangles)), **(D)** concentrations of CFPS reagents for cytoplasm mimicry (Cytomim; putrescine (white circles) and spermidine (orange circles)), and (**E**) K_2PO_4 concentrations (a proxy for phosphate generated during CFPS). Concentrations of CFPS reagents are varied as 'X Concentration in CFPS' where '1' would be the concentration of that reagent when a typical CFPS reaction is run. Each error bar represents standard deviations of technical replicates with n ≥ 3. (For interpretation of the references to color in this figure legend, the reader is referred to the web version of this article.)

classes: (1) components involved in transcription-translation (*e.g.,* amino acids, nucleotides), (2) components that mimic the cytoplasm (*e.g.,* putrescine, spermidine), and (3) components that modulate metabolism (*e.g.,* phosphoenolpyruvate (PEP), oxalate). We assessed the impact of supplementing CFME *n*-butanol synthesis reactions with components from each of these classes at increasing concentrations. The addition of transcription-translation substrates (nucleotides and amino acids, respectively) at 1X CFPS concentrations decreases *n*-butanol production by ~ 20% as compared to the standard CFME reaction (Fig. 4**B**). The 'cytomimicry' components, spermidine and putrescine, decrease *n*-butanol synthesis levels by ~ 18% at 1X CFPS concentrations and remain at these levels at higher concentrations of spermidine and putrescine (Fig. 4**D**). In contrast, the metabolites involved in energy regeneration, oxalate and PEP, greatly reduce *n*-butanol production (Fig. 4**C**). These trends are supported by corresponding levels of lactate and acetate (Supplementary Fig. 3). As a potent inhibitor of phosphoenolpyruvate synthetase, we suspect that oxalate impacted the metabolic network around pyruvate and PEP to redirect flux resulting in lower levels of *n*-butanol. While each component tested influences *n*-butanol synthesis, during CFPS-ME these components exist at < 0.5X concentrations during the reactions and likely do not individually cause drastic effects on *n*-butanol synthesis.

While PEP at < 0.5X concentrations seems to not be detrimental, we know that PEP is used as a secondary energy source to regenerate ATP for energizing protein synthesis causing the concomitant release of free inorganic phosphate. We wanted to therefore test the effect of inorganic phosphate as we also know that phosphate can inhibit translation by sequestering magnesium (Anderson et al., 2015) and could be deleterious to *n*-butanol synthesis as it does have an effect on glycolysis (Calhoun and Swartz, 2005). To test this hypothesis, we evaluated the addition of 0–80 mM inorganic phosphate in the form of potassium phosphate to our glucose-driven CFME *n*-butanol biosynthesis system at the start of the reaction (Fig. 4**E**). We observed that *n*-butanol production has a phosphate optimum between 10 and 20 mM phosphate added to the system, but that high concentrations that would be representative of the CFPS-ME system (*i.e.,* > 30 mM) were inhibitory relative to the optimum (~ 15% reduction). These observations re-inforce previous studies that have shown that inorganic phosphate, when operating glycolysis, is a key component for optimizing cell-free systems (Calhoun and Swartz, 2005; Jewett et al., 2008). In sum, our analysis suggests each of the CFPS reagents together cause the reduction in *n*-butanol synthesis and that accumulated phosphate from PEP could be a major player in altering metabolism. By leveraging the ability to probe each physiochemical reagent afforded by the cell-free system we are able to parse individual and synergistic effects of physiochemical conditions on metabolism.

3.3. Non-phosphorylated energy sources decrease phosphate accumulation and shed light on the pH dependence of n-butanol synthesis

Readily altering physiochemical parameters gave us the ability to optimize *n*-butanol production in a cell-free system as well as observe differences between two cell-free systems (CFME and CFPS-ME) correlated with the addition of CFPS reagents. One result we observed was that phosphate is accumulated in CFPS-coupled systems (Fig. 4**E**). This is due to the catabolism of PEP during CFPS. While the addition of PEP and each CFPS small molecule reagent contributes to productive protein synthesis, many alternative energy sources have been used to fuel CFPS such as glucose, pyruvate, and polysugars (Calhoun and Swartz, 2005; Jewett et al., 2008; Wang and Zhang, 2009; Caschera and Noireaux, 2015, 2014; Knapp et al., 2007). We hypothesized that alternative non-phosphorylated secondary energy sources for CFPS, instead of PEP, might mitigate the detrimental effect of phosphate on *n*-butanol metabolism. We tested five energy sources for CFPS during CFPS-ME each at varying metabolic nodes away from acetyl-CoA (PEP, pyruvate, glucose, maltose, and maltodextrin) (Supplementary Fig. 4).

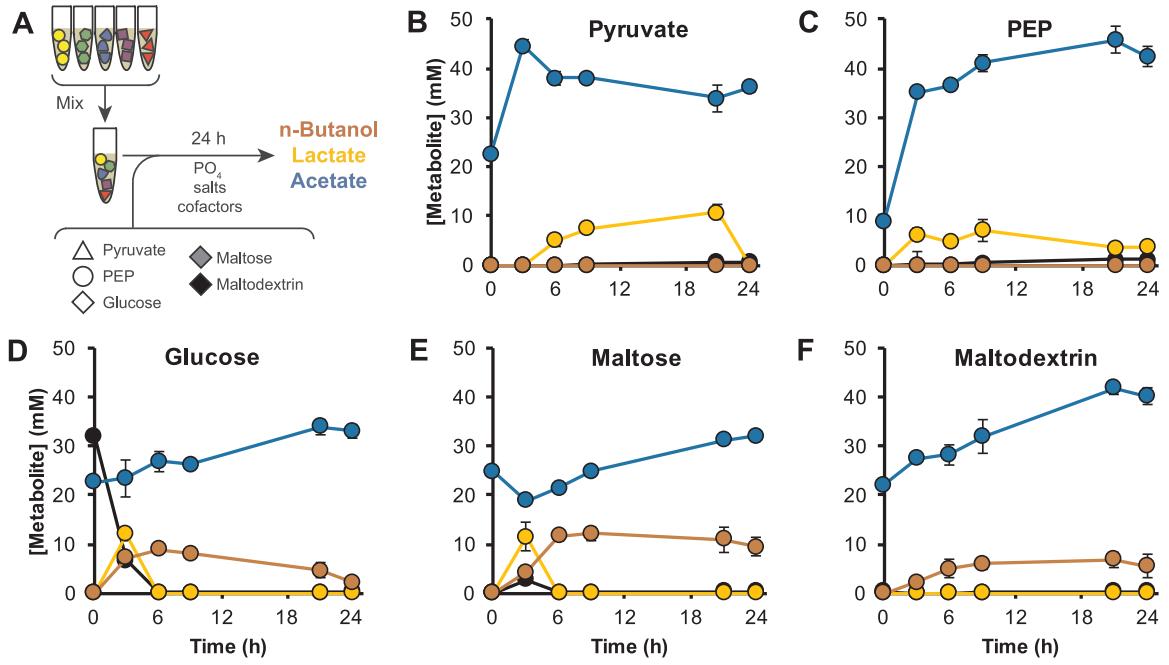

Fig. 5. Cell-free CFME reactions can be run from alternative energy substrates to produce *n*-butanol. (A) Cell-free CFME reactions were run with five extracts mixed to have all *n*-butanol pathway enzymes present with the addition of biosynthetic pathway starting substrates and cofactors and incubation for 24 h at 30 °C. Glucose (black), lactate (yellow), acetate (blue), and *n*-butanol (orange) were measured at 0, 3, 6, 9, 21, and 24 h. Metabolite (glucose, lactate, acetate, *n*-butanol) profiles are shown for reactions testing 33 mM (**B**) pyruvate, (**C**) PEP, (**D**) glucose, (**E**) maltose, and (**F**) maltodextrin as biosynthetic pathway starting substrates. Each error bar represents standard deviations of technical replicates with n ≥ 3. (For interpretation of the references to color in this figure legend, the reader is referred to the web version of this article.)

Unsurprisingly, PEP is the best energy source for protein synthesis, which makes sense because the physiochemical reagents in our CFPS system have been optimized for use with PEP. Additionally, PEP is the only source that accumulates > 10 mM phosphate in the system as it is a direct phosphate donor. Further optimization of reagents could be useful for CFPS-ME using these alternative energy sources.

Being able to quickly adjust new reagents in cell-free systems, we next tested the same five energy sources as the sole substrate to fuel CFME *n*-butanol synthesis (Fig. 5**A**). We observed that 33 mM pyruvate and PEP are unable to produce *n*-butanol (Fig. 5**B–C**), likely because their conversion does not provide enough NADH driving force that would normally come from glycolysis to make *n*-butanol. Using 33 mM glucose, maltose, and maltodextrin produce *n*-butanol with similar profiles but at different rates (Fig. 5**D–F**). This makes sense because each substrate is similarly catabolized during glycolysis, but maltose and maltodextrin must first be broken into glucose monomers. In addition, 33 mM maltose and maltodextrin is essentially twice as much carbon substrate as 33 mM glucose which likely plays a role in the difference between the *n*-butanol synthesis rates.

We can also compare alternative energy substrates by observing accumulated phosphate and corresponding pH levels (Fig. 6). Using PEP for CFME accumulates the most phosphate with pyruvate and maltodextrin also accumulating phosphate (Fig. 6**B**). These systems all produce the least amount of *n*-butanol and further support the need to maintain low phosphate levels. Most interestingly, the pH of the system correlates with the amount of *n*-butanol that is produced (lower pH's correspond with higher *n*-butanol titers) (Fig. 6**C**). This correlation could be due to low pH being beneficial for *n*-butanol synthesis or due to the increase in amount of energy metabolized (polysugar substrates) leading to increased *n*-butanol synthesis and thus lower pH. It is important to note that the compounds tested differ greatly in the amount of carbon supplied as substrate and metabolized as already mentioned. In addition, higher concentrations (120 mM) of glucose correlate with a decrease in pH indicated by black X's in Fig. 6**C**, which makes sense as more glucose means four-times more carbon and therefore a more active metabolism. However, in congruence with previous reports of *Clostridium* metabolism, *n*-butanol production is optimal below pH of 7 (Yu et al., 2015; Dusséaux et al., 2013; Lutke-Eversloh and Bahl, 2011), suggesting that the low pH may indeed be beneficial for *n*-butanol synthesis. For CFME, using alternative buffers could alleviate limitations in *n*-butanol production. For CFPS, pH 7–8 is optimal for protein synthesis (Jewett and Swartz, 2004). Together these results shed light on the essential physiochemical limitations of CFPS-ME for *n*-butanol synthesis only accessible by the physiochemical levers of crude-lysate systems. Moreover, they suggest that separating protein synthesis from *n*-butanol biosynthesis, a two-pot system, might improve pathway performance and its study.

4. Discussion

In this study, we present an approach to use crude extract-based cell-free systems to study biosynthetic pathway performance by physiochemical perturbations. First, we explored the backdrop of physiochemical parameters important for *n*-butanol production using liquid-handling robotics, which enabled physiochemical landscapes to be mapped for optimizing pathway performance. This optimization improved cell-free *n*-butanol synthesis yields and demonstrates a generalizable strategy to inform biosystems design by modulating metabolism dynamics. Second, we compared and modified cell-free metabolic profiles in biosynthetic systems derived from (i) mix-and-match crude lysates where enzymes are made in cells prior to lysis (CFME) and from (ii) CFPS-coupled systems where enzymes are made post-lysis (CFPS-ME). This taught us that the physiochemical complexity of an all-in-one CFPS-ME system inhibits *n*-butanol production and that physiochemical conditions play a major role in directing metabolism. Third, and to alleviate phosphate inhibition, we tested the impact of using non-phosphorylated energy substrates on cell-free pathway performance. We observed that CFME reactions fueled by PEP and pyruvate had higher accumulated phosphate levels and higher pH's (~ 8) as compared to reactions with glucose, maltose, and maltodextrin (~ 7). While this correlation between pH and *n*-butanol synthesis is noteworthy, the causal relationship is still unfounded. Whether using

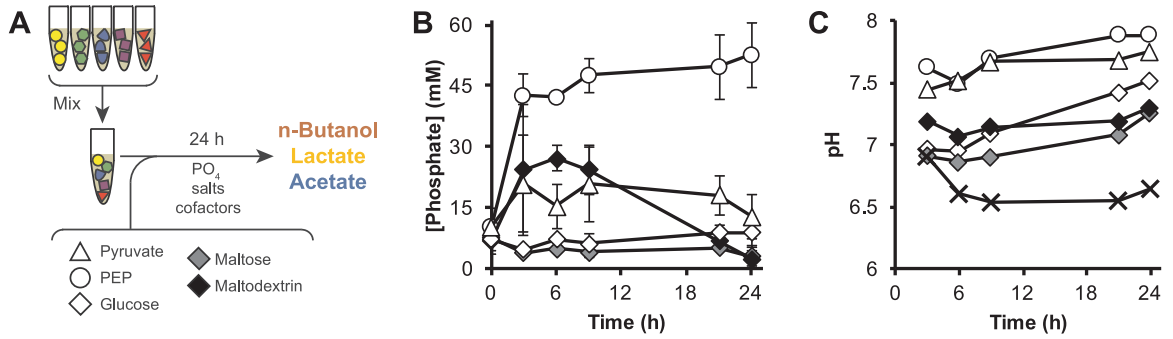

Fig. 6. Using alternative energy substrates for CFME show varied operating phosphate and pH. (A) Cell-free CFME reactions were run with five extracts mixed to have all *n*-butanol pathway enzymes present with the addition of biosynthetic pathway starting substrates and cofactors and incubation for 24 h at 30 °C. Phosphate levels and pH were measured at 0, 3, 6, 9, 21, and 24 h. (**B**) Accumulated phosphate and (**C**) pH profiles are shown for reactions testing 33 mM pyruvate (white triangle), PEP (white circle), glucose (white diamond), maltose (grey diamond), and maltodextrin (black diamond) as biosynthetic pathway starting substrates. The pH of a CFME control reaction (120 mM glucose) is measured (black Xs) in (**C**). Each error bar represents standard deviations of technical replicates with n ≥ 3.

33 mM maltose rather than 33 mM glucose, which is effectively twice as much carbon, would result in more *n*-butanol synthesis because of a lower pH or more *n*-butanol because of the increase in carbon supplied and catabolized is an open question. Luckily, our framework would allow manual adjustment of pH, carbon substrate, and by-products during reactions to test the causal nature of these types of relationships. Taken together, the modular nature of our approach is poised to facilitate multiplexed, automated study of biosynthetic pathways to inform systems design.

Having demonstrated the utility of modifying and controlling the physiochemical environment for cell-free biosynthetic systems, we interestingly found that lower system pH corresponded with increased *n*-butanol levels consistent with optimal pH's for *n*-butanol synthesis in native producers (Yu et al., 2015; Dusséaux et al., 2013; Lutke-Eversloh and Bahl, 2011). With this in mind and the flexibility to alter the physiochemical background, future work will focus on mimicking the cellular environment during different phases of growth to study pathway performance. For example, *Clostridium* undergo a biphasic metabolism during acetone-butanol-ethanol (ABE) fermentation. First the bacteria grow exponentially during the acidogenesis phase of metabolism. Then the bacteria enter stationary phase which corresponds with a switch to solventogenesis. These two phases represent two different metabolic profiles, pH's, and pathway operations. Just as we altered the physiochemical conditions of the cell-free systems to change the profiles of *n*-butanol, acetate, and lactate, one could imagine changing the physiochemical environment to mirror acidogenesis and solventogenesis to more accurately reflect pathway behavior. This could provide a more robust analysis of pathway dynamics to inform how pathways of enzymes operate during different bacterial growth regimes.

There are several applications of cell-free systems that the ability to control the physiochemical environment would facilitate. Most notably are the use of cell-free systems to study cellular metabolism, screen biosynthetic pathways for cellular metabolic engineering, and develop cell-free biomanufacturing platforms. The tools and analysis performed in this work lays the groundwork to both rapidly prototype biosynthesis for *in vivo* use and to optimize pathways for *in vitro* use. Towards these applications it is important to have a robust and reliable cell-free setup. While there is variability of biosynthesis due to the accuracy of liquid-handling robotics, these systems are highly reproducible. Cell-free protein synthesis systems routinely perform well across lysates made from separate *E. coli* cultures (Kwon and Jewett, 2015). Across the separate sets of mixed lysates (made from separate cultures of *E. coli*), the variability in *n*-butanol production after 24 h is insignificant (Supplementary Fig. 5). Cell-free systems would thus be able to hold up to the strains of high-throughput testing as well as stable biomanufacturing. Recent work from the Bowie laboratory, for example, shows the robust ability to control cofactor and redox balance for biomanufacturing (Opgenorth et al., 2016; Opgenorth et al., 2017). These works and the study we present here show how managing the physiochemical environment can facilitate metabolic engineering efforts.

Physiochemical manipulability makes cell-free metabolism highly controllable. We can use this feature to alter metabolism, tune and recover differences between cell-free biosynthetic systems, and potentially mimic different growth phase metabolisms and non-model organisms. While CFPS-coupled crude-lysate biosynthetic systems offer the best cell-free route to accelerate metabolic engineering DBT iterations, an important conclusion from our work is that there exists a dichotomy between the optimal physiochemical conditions for CFPS and those for biosynthetic pathway operation. This suggests that CFPS-coupled biosynthetic systems would be more powerful prototyping tools if multi-pot, phosphate-minimal, pH-controlled systems were developed. Looking forward, we expect to see the development of cell-free biosynthetic systems developed as multiple “unit operations” that can be individually optimized and assayed gaining precise control over biosynthetic pathway construction. This concept of “unit operations”, borrowed from chemical engineering, would offer even greater control over protein and metabolite synthesis allowing for better discernment of variation in metabolism due to changes in enzyme, making possible high resolution strategies to prototype biosynthetic enzymes and pathways to speed up metabolic engineering DBT cycles.

Acknowledgments

We graciously thank the Department of Energy (BER grant: DE-SC0018249), the David and Lucile Packard Foundation (2011-37152), and the Dreyfus Teacher-Scholar Program for support. A.S.K. is an NSF Graduate Fellow.

Author contributions

A.S.K. and M.C.J. conceived and designed the experiments. A.S.K., J.T.H., and S.A.C. performed all of the experimental work. A.S.K. and M.C.J. wrote the manuscript.

Competing financial interests

The authors declare no competing financial interests.

Appendix A. Supplementary material

Supplementary data associated with this article can be found in the online version at http://dx.doi.org/10.1016/j.ymben.2017.11.005.

References

Anderson, M.J., Stark, J.C., Hodgman, C.E., Jewett, M.C., 2015. Energizing eukaryotic cell-free protein synthesis with glucose metabolism. FEBS Lett. 589, 1723–1727. http://dx.doi.org/10.1016/j.febslet.2015.05.045.

Bogorad, I.W., Lin, T.S., Liao, J.C., 2013. Synthetic non-oxidative glycolysis enables complete carbon conservation. Nature 502, 693–697. http://dx.doi.org/10.1038/nature12575.

Boyle, P.M., Silver, P.A., 2012. Parts plus pipes: synthetic biology approaches to metabolic engineering. Metab. Eng. 14, 223–232. http://dx.doi.org/10.1016/j.ymben.2011.10.003.

Bujara, M., Schumperli, M., Pellaux, R., Heinemann, M., Panke, S., 2011. Optimization of a blueprint for in vitro glycolysis by metabolic real-time analysis. Nat. Chem. Biol. 7, 271–277. http://dx.doi.org/10.1038/nchembio.541.

Calhoun, K.A., Swartz, J.R., 2005. Energizing cell-free protein synthesis with glucose metabolism. Biotechnol. Bioeng. 90, 606–613. http://dx.doi.org/10.1002/bit.20449.

Caschera, F., Noireaux, V., 2014. Synthesis of 2.3 mg ml^{-1} of protein with an all Escherichia coli cell-free transcription–translation system. Biochimie 99, 162–168. http://dx.doi.org/10.1016/j.biochi.2013.11.025.

Caschera, F., Noireaux, V., 2015. A cost-effective polyphosphate-based metabolism fuels an all E. coli cell-free expression system. Metab. Eng. 27, 29–37. http://dx.doi.org/10.1016/j.ymben.2014.10.007.

Caspi, R., et al., 2014. The MetaCyc database of metabolic pathways and enzymes and the BioCyc collection of Pathway/Genome Databases. Nucleic Acids Res. 42, D459–D471. http://dx.doi.org/10.1093/nar/gkt1103.

Chang, A., et al., 2015. BRENDA in 2015: exciting developments in its 25th year of existence. Nucleic Acids Res. 43, D439–D446. http://dx.doi.org/10.1093/nar/gku1068.

Dong, H., et al., 2015. Engineering Escherichia coli cell factories for n-Butanol production. Adv. Biochem. Eng./Biotechnol. http://dx.doi.org/10.1007/10_2015_306.

Dudley, Q.M., Karim, A.S., Jewett, M.C., 2015. Cell-free metabolic engineering: biomanufacturing beyond the cell. Biotechnol. J. 10, 69–82. http://dx.doi.org/10.1002/biot.201400330.

Dudley, Q.M., Anderson, K.C., Jewett, M.C., 2016. Cell-free mixing of Escherichia coli crude extracts to prototype and rationally engineer high-titer mevalonate synthesis. ACS Synth. Biol. http://dx.doi.org/10.1021/acssynbio.6b00154.

Dusséaux, S., Croux, C., Soucaille, P., Meynial-Salles, I., 2013. Metabolic engineering of Clostridium acetobutylicum ATCC 824 for the high-yield production of a biofuel composed of an isopropanol/butanol/ethanol mixture. Metab. Eng. 18, 1–8. http://dx.doi.org/10.1016/j.ymben.2013.03.003.

Garamella, J., Marshall, R., Rustad, M., Noireaux, V., 2016. The All E. coli TX-TL toolbox 2.0: a platform for cell-free synthetic biology. ACS Synth. Biol. 5, 344–355. http://dx.doi.org/10.1021/acssynbio.5b00296.

Goering, A.W., et al., 2016. In vitro reconstruction of nonribosomal peptide biosynthesis directly from DNA using cell-free protein synthesis. ACS Synth. Biol. http://dx.doi.org/10.1021/acssynbio.6b00160.

Hold, C., Billerbeck, S., Panke, S., 2016. Forward design of a complex enzyme cascade reaction. Nat. Commun. 7, 12971. http://dx.doi.org/10.1038/ncomms12971.

Hong, S.H., et al., 2014. Cell-free protein synthesis from a release factor 1 deficient Escherichia coli activates efficient and multiple site-specific nonstandard amino acid incorporation. ACS Synth. Biol. 3, 398–409. http://dx.doi.org/10.1021/sb400140t.

Jewett, M.C., Swartz, J.R., 2004. Mimicking the Escherichia coli cytoplasmic environment activates long-lived and efficient cell-free protein synthesis. Biotechnol. Bioeng. 86, 19–26. http://dx.doi.org/10.1002/bit.20026.

Jewett, M.C., Calhoun, K.A., Voloshin, A., Wuu, J.J., Swartz, J.R., 2008. An integrated cell-free metabolic platform for protein production and synthetic biology. Mol. Syst. Biol. 4, 220. http://dx.doi.org/10.1038/msb.2008.57.

Karim, A.S., Jewett, M.C., 2016. A cell-free framework for rapid biosynthetic pathway prototyping and enzyme discovery. Metab. Eng. 36, 116–126. http://dx.doi.org/10.1016/j.ymben.2016.03.002.

Kay, J.E., Jewett, M.C., 2015. Lysate of engineered Escherichia coli supports high-level conversion of glucose to 2,3-butanediol. Metab. Eng. 32, 133–142. http://dx.doi.org/10.1016/j.ymben.2015.09.015.

Keasling, J.D., 2010. Manufacturing molecules through metabolic engineering. Science 330, 1355–1358. http://dx.doi.org/10.1126/science.1193990.

Keasling, J.D., 2012. Synthetic biology and the development of tools for metabolic engineering. Metab. Eng. 14, 189–195. http://dx.doi.org/10.1016/j.ymben.2012.01.004.

Kelwick, R., Webb, A.J., MacDonald, J.T., Freemont, P.S., 2016. Development of a Bacillus subtilis cell-free transcription-translation system for prototyping regulatory elements. Metab. Eng. 38, 370–381. http://dx.doi.org/10.1016/j.ymben.2016.09.008.

Knapp, K.G., Goerke, A.R., Swartz, J.R., 2007. Cell-free synthesis of proteins that require disulfide bonds using glucose as an energy source. Biotechnol. Bioeng. 97, 901–908. http://dx.doi.org/10.1002/bit.21296.

Kwok, R., 2010. Five hard truths for synthetic biology. Nature 463, 288–290. http://dx.doi.org/10.1038/463288a.

Kwon, Y.C., Jewett, M.C., 2015. High-throughput preparation methods of crude extract for robust cell-free protein synthesis. Sci. Rep. 5, 8663. http://dx.doi.org/10.1038/srep08663.

Lee, J.W., et al., 2012. Systems metabolic engineering of microorganisms for natural and non-natural chemicals. Nat. Chem. Biol. 8, 536–546. http://dx.doi.org/10.1038/nchembio.970.

Lutke-Eversloh, T., Bahl, H., 2011. Metabolic engineering of Clostridium acetobutylicum: recent advances to improve butanol production. Curr. Opin. Biotechnol. 22, 634–647. http://dx.doi.org/10.1016/j.copbio.2011.01.011.

Moore, S.J., Lai, H.E., Needham, H., Polizzi, K.M., Freemont, P.S., 2017. Streptomyces venezuelae TX-TL - a next generation cell-free synthetic biology tool. Biotechnol. J. 12. http://dx.doi.org/10.1002/biot.201600678.

Morgado, G., Gerngross, D., Roberts, T.M., Panke, S., 2016. Synthetic biology for cell-free biosynthesis: fundamentals of designing novel in vitro multi-enzyme reaction networks. Adv. Biochem. Eng./Biotechnol. http://dx.doi.org/10.1007/10_2016_13.

Na, D., Kim, T.Y., Lee, S.Y., 2010. Construction and optimization of synthetic pathways in metabolic engineering. Curr. Opin. Microbiol. 13, 363–370. http://dx.doi.org/10.1016/j.mib.2010.02.004.

Nielsen, J., Keasling, J.D., 2016. Engineering cellular metabolism. Cell 164, 1185–1197. http://dx.doi.org/10.1016/j.cell.2016.02.004.

Opgenorth, P.H., Korman, T.P., Bowie, J.U., 2016. A synthetic biochemistry module for production of bio-based chemicals from glucose. Nat. Chem. Biol. 12, 393–395. http://dx.doi.org/10.1038/nchembio.2062.

Opgenorth, P.H., Korman, T.P., Iancu, L., Bowie, J.U., 2017. A molecular rheostat maintains ATP levels to drive a synthetic biochemistry system. Nat. Chem. Biol. 13, 938–942. http://dx.doi.org/10.1038/nchembio.2418.

Paddon, C.J., Keasling, J.D., 2014. Semi-synthetic artemisinin: a model for the use of synthetic biology in pharmaceutical development. Nat. Rev. Microbiol 12, 355–367. http://dx.doi.org/10.1038/nrmicro3240.

Sun, Z.Z., Yeung, E., Hayes, C.A., Noireaux, V., Murray, R.M., 2014. Linear DNA for rapid prototyping of synthetic biological circuits in an Escherichia coli based TX-TL cell-free system. ACS Synth. Biol. 3, 387–397. http://dx.doi.org/10.1021/sb400131a.

Takahashi, M.K., et al., 2015. Characterizing and prototyping genetic networks with cell-free transcription–translation reactions. Methods 86, 60–72. http://dx.doi.org/10.1016/j.ymeth.2015.05.020.

Wang, Y., Zhang, Y.H., 2009. Cell-free protein synthesis energized by slowly-metabolized maltodextrin. BMC Biotechnol. 9, 58. http://dx.doi.org/10.1186/1472-6750-9-58.

Yu, L., Xu, M., Tang, I.C., Yang, S.T., 2015. Metabolic engineering of Clostridium tyrobutyricum for n-butanol production through co-utilization of glucose and xylose. Biotechnol. Bioeng. 112, 2134–2141. http://dx.doi.org/10.1002/bit.25613.

Zhu, F., et al., 2014. In vitro reconstitution of mevalonate pathway and targeted engineering of farnesene overproduction in Escherichia coli. Biotechnol. Bioeng. 111, 1396–1405. http://dx.doi.org/10.1002/bit.25198.